

# GaMnAs: Position of Mn-*d* levels and majority spin band gap predicted from GGA-1/2 calculations

Cite as: Appl. Phys. Lett. **100**, 202408 (2012); <https://doi.org/10.1063/1.4718602>

Submitted: 03 February 2012 • Accepted: 24 April 2012 • Published Online: 17 May 2012

R. R. Pelá, M. Marques, L. G. Ferreira, et al.



## ARTICLES YOU MAY BE INTERESTED IN

Slater half-occupation technique revisited: the LDA-1/2 and GGA-1/2 approaches for atomic ionization energies and band gaps in semiconductors

AIP Advances **1**, 032119 (2011); <https://doi.org/10.1063/1.3624562>

Digital magnetic heterostructures based on GaN using GGA-1/2 approach

Applied Physics Letters **101**, 112403 (2012); <https://doi.org/10.1063/1.4751285>

Recent progress in III-V based ferromagnetic semiconductors: Band structure, Fermi level, and tunneling transport

Applied Physics Reviews **1**, 011102 (2014); <https://doi.org/10.1063/1.4840136>



## Characterizing nanostructures?

Learn about a new way to get high-quality data in a fraction of the time

Read the tech note



# GaMnAs: Position of Mn-*d* levels and majority spin band gap predicted from GGA-1/2 calculations

R. R. Pelá,<sup>1,a)</sup> M. Marques,<sup>1</sup> L. G. Ferreira,<sup>1,2</sup> J. Furthmüller,<sup>3</sup> and L. K. Teles<sup>1</sup>

<sup>1</sup>Instituto Tecnológico de Aeronáutica, 12228-900 São José dos Campos, SP, Brazil

<sup>2</sup>Instituto de Física, Universidade de São Paulo, CP 66318, 05315-970 São Paulo, SP, Brazil

<sup>3</sup>Institut für Festkörpertheorie und-optik, Friedrich-Schiller-Universität, 07743 Jena, Germany

(Received 3 February 2012; accepted 24 April 2012; published online 17 May 2012)

Among all magnetic semiconductors, GaMnAs seems to be the most important one. In this work, we present accurate first-principles calculations of GaMnAs within the GGA-1/2 approach: We concentrate our efforts in obtaining the position of the peak of Mn-*d* levels in the valence band and also the majority spin band gap. For the position of the Mn-*d* peak, we find a value of 3.3 eV below the Fermi level, in good agreement with the most recent experimental results of 3.5 and 3.7 eV. An analytical expression that fits the calculated  $E_g(x)$  for majority spin is derived in order to provide ready access to the band gap for the composition range from 0 to 0.25. We found a value of 3.9 eV for the gap bowing parameter. The results agree well with the most recent experimental data.

© 2012 American Institute of Physics. [<http://dx.doi.org/10.1063/1.4718602>]

Recently, there has been increasing interest in exploring the spin degree of freedom in addition to the charge in semiconductors by the emerging field of semiconductor spintronics.<sup>1</sup> Spin devices are expected to have great advantages to their charge counterparts, being faster, smaller, and less energy consuming.<sup>1,2</sup> In the last 20 years, enormous efforts have been made toward the achievement of an ideal magnetic semiconductor (MS), formed by alloying magnetic elements and semiconductors, because this allows an interplay between magnetic and electronic properties<sup>3</sup> and could make semiconductor circuits behave as storage circuits.<sup>4</sup>

Among the possible choices for MSs, GaMnAs is one of the most outstanding materials.<sup>5</sup> It is the only material for which magnetic hysteresis, polarized light emission, and the anomalous Hall effect have been reported.<sup>6</sup> In GaMnAs, Mn substitutes Ga and furnishes a magnetic moment to the MS (since it has five electrons in the open 3*d* shell), and at the same time it acts as an acceptor. Experiments have shown that the valence-band holes (that appear due to the presence of Mn) are crucial to sustain the ferromagnetism in the alloy. At the same time they permit an electrical control of the magnetic properties.<sup>4</sup> All these features make GaMnAs a very interesting material to be investigated.

On the other hand, from a theoretical point of view, first-principles calculations can provide useful information about structural, thermodynamic, and electronic properties. The majority of these calculations is based on density functional theory (DFT) combined with the local density approximation (LDA) or with the generalized gradient approximation (GGA) for the exchange-correlation (XC) functional. However, some properties, such as the magnetic ones or the electronic band structures, can depend quite sensitively on the XC approximation employed.<sup>4</sup> The band gap, which is a fundamental property of a semiconductor, is always underestimated in both LDA and GGA approaches. Also, the nonlocality of the (screened) exchange interaction is not taken into account, and the electrostatic self-

interaction is not entirely compensated: This lack of compensation causes large errors for localized states, such as Mn-*d* states,<sup>7</sup> tending to place these states at too high energies in comparison with the top of valence band. It is now widely accepted that some correction is needed for Mn-*d* levels in GaMnAs.<sup>4,8</sup>

Several methods for overcoming these limitations have been proposed. One of them is the GW approximation, in which one considers the energies of quasi-particles and calculates the electron self-energy in terms of perturbation theory.<sup>9</sup> This procedure has been quite successful achieving good accuracy, but it is computationally very demanding, and this is a major obstacle to employ such an approach to simulate MSs with low magnetic atom content because of the need of a large supercell. Other procedures have also been proposed; among them, we can mainly cite the self interaction correction (SIC),<sup>10</sup> hybrid functionals,<sup>11</sup> screened exchange (SX-LDA),<sup>12</sup> the so-called exact-exchange approach,<sup>13</sup> the well known LDA+*U*,<sup>14</sup> etc. For GaMnAs, it is well known that LDA+*U* can provide better results.<sup>4</sup> In this approach, the Hubbard description of strongly correlated orbitals is combined with DFT, and one additional parameter *U* is added to the energy functional. However, this *U* parameter is not known in principle and should be obtained by fitting the results to some reported measurements. The value of *U* that is needed for Mn-*d* orbital is not well defined as well: Some studies report a value of 3 eV,<sup>15</sup> while others claim it to be 4 eV.<sup>16</sup> Moreover, the LDA+*U* cannot be applied to all magnetic compounds since the wider gap GaMnN MS is not well described by this approach.<sup>8</sup>

Recently Ferreira *et al.*<sup>17</sup> have developed a simple and successful procedure, with no adjustable parameters, to calculate the excitation energy spectrum. The procedure is inspired by the old Slater transition state technique for atoms, shown to be equivalent to the inclusion of the self-energy of the quasi-particle. The self-energy potential is calculated for the atom, and, when transferred to an infinite crystal, it is trimmed not to extend to neighboring atoms. The trimming is made by means of a cutting function with a

<sup>a)</sup>Electronic mail: rrpela@ita.br.

parameter “CUT” which is determined variationally by making the band gap extreme. As with the best GW calculations, the Ferreira *et al.* method, named LDA-1/2, produces very good band gaps and effective masses, but at a very small computational price. It is capable to treat a great variety of compounds ranging from small gap semiconductors such as InSb to large gap such as SiO<sub>2</sub>. Lately we have been also using a GGA-1/2 method, where the exchange-correlation is GGA, instead of LDA, and the  $-1/2$  is to remind that we remove 1/2 electron, as in the transition state technique. LDA-1/2 and also GGA-1/2 have proven to describe correctly the excitation aspects in binary compounds,<sup>17,18</sup> alloys,<sup>19</sup> and interfaces.<sup>20</sup>

In this article, we perform *ab initio* calculations based on DFT using both GGA-1/2 and GGA for the XC potential to contrast the results. The Kohn-Sham equations are solved by employing the projector augmented waves (PAW) scheme as implemented in the Viena *ab initio* Simulation Package (VASP).<sup>21,22</sup> Before we simulate GaMnAs, we consider the binary compound GaAs just to reveal the accuracy of the GGA-1/2 method. By using the GaAs experimental lattice constant<sup>23</sup> of 5.64 Å, we obtain a gap of 0.484 eV for GGA and of 1.475 eV for GGA-1/2. The latter gap value fits nicely to the measured gap,<sup>23</sup> which is 1.519 eV. The spin-orbit splitting  $\Delta_{SO} = 0.332$  eV is the same for both GGA and GGA-1/2 approaches and agrees with the experimental value of 0.341 eV.<sup>23</sup>

Initially, we focus our attention on obtaining the right position of Mn-*d* levels. In this first moment, we consider a Mn composition  $x = 6.25\%$  and make use of a supercell containing 32 atoms (16 cations and 16 anions), in which one Mn atom substitutes one Ga atom. All Mn spin moments are forced to be aligned ferromagnetically. The supercell employed in our calculations is depicted in Fig. 1: It has a body centered cubic symmetry and its primitive vectors are given by  $\vec{a}_1 = a(-1, 1, 1)$ ,  $\vec{a}_2 = a(1, -1, 1)$ , and  $\vec{a}_3 = a(1, 1, -1)$ , where  $a$  is the lattice parameter. The experimental lattice constant<sup>24</sup>  $a = 5.68$  Å for this Mn composition was used in our calculations.

In the GGA-1/2 calculation, like in the LDA-1/2 calculation, we must determine the CUT parameter before the intended calculation. In our case, to correctly describe the

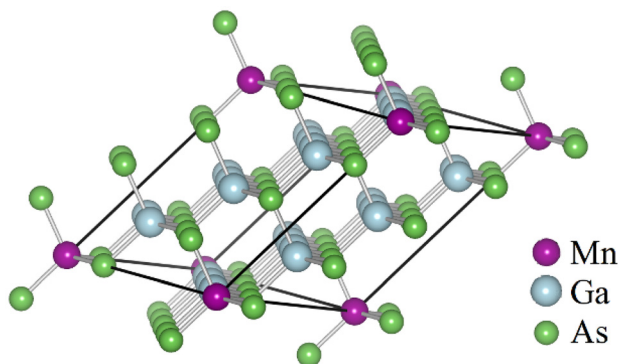


FIG. 1. Body centered cubic supercell of 32 atoms. The geometrical limits of this supercell appear highlighted with a thick black line. Although the system crystallizes in the zinc-blende structure, this supercell is the most symmetric one to simulate 32 atoms in the zinc-blende configuration.

TABLE I. Half-ionized orbitals used in the GGA-1/2 method. The CUT is given in atomic units.

Atom	Orbital	CUT
As	4 <i>p</i>	3.81
Ga	3 <i>d</i>	1.23
Mn	3 <i>d</i>	3.00

electronic states of GaMnAs, we need to employ the half-ionized correction for the As 4*p*, Ga 3*d*, and also Mn 3*d* levels. We use the same GGA-1/2 CUTs for As and Ga as those ones mentioned in Ref. 17, since CUT has proven to be a transferable quantity.<sup>17</sup> On the other hand, for the Mn 3*d*, there is no standard technique to determine CUT since it is obtained for semiconducting materials making the band gap extreme. Here, we only consider the majority spin band gap for Ga<sub>0.9375</sub>Mn<sub>0.0625</sub>As and find the CUT parameter shown in Table I. We noted that considering only the *d* levels for the one of this paper and Ref. 17, the CUT parameter has a linear behavior with the 90% atomic charge radii as one can be observed in Fig. 2, reinforcing the atomic character of the *d* levels. This result, perhaps, can lead to another method for obtaining the CUT although more tests must be performed to confirm it.

We show in Fig. 3 the spin-decomposed density of states (DOS) for a standard GGA calculation (a) and for a GGA-1/2 calculation (b). Our GGA DOS compares well with other theoretical calculations performed within the LDA approach.<sup>16,25–28</sup> The first thing to note is that GGA predicts a small gap for both spin-up and spin-down (where the spin-up gap appears above the Fermi level, inside unoccupied states; only for spin-down the Fermi level occurs inside the gap demonstrating the half-metallic character). This gap underestimation is usual for GGA. The GGA-1/2 correction opens these gaps. Also, the Mn-*d* bands become narrower in GGA-1/2 than in GGA, resulting in more localized *d* states, as expected. The spin-up states between the Fermi level (0 eV) and  $-0.4$  eV are formed by Mn-*d* *t*<sub>2</sub> states and *p* orbitals of the four As first neighbors of Mn. This is consistent

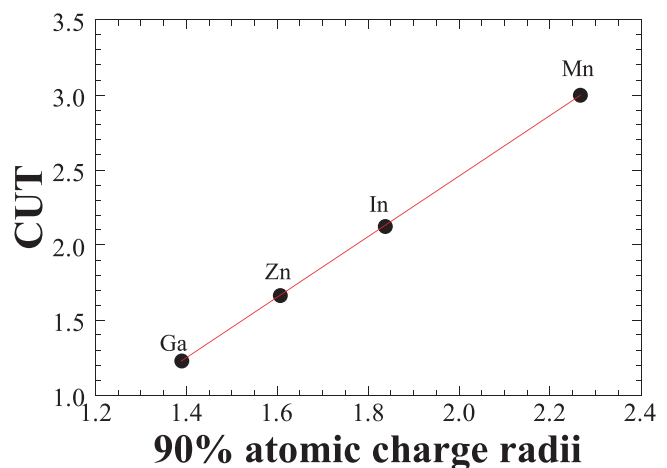


FIG. 2. CUT values for levels-*d* obtained by the standard procedure as a function of 90% atomic charge radii  $R$ . The fitting curve results on  $CUT = -1.57 + 2.02R$ .

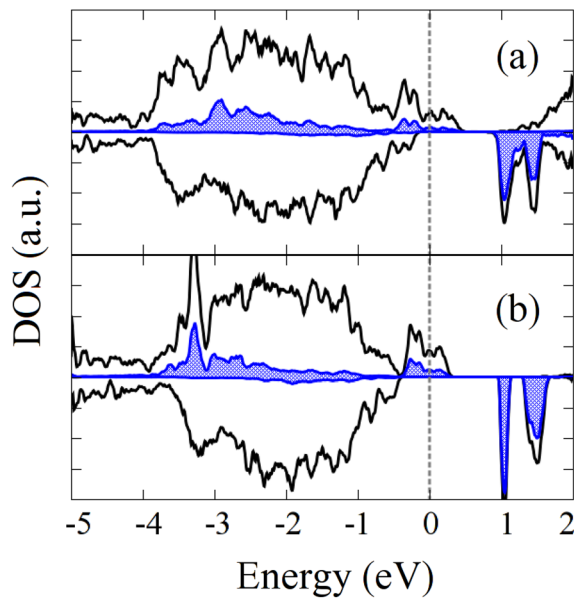


FIG. 3. DOS calculated within (a) GGA and (b) GGA-1/2. All the energy values are referred to the Fermi level, depicted as the gray dotted line. The black line is the total DOS while the filled blue line is the Mn-*d* projected DOS.

with experimental observations.<sup>29,30</sup> However, we note that these states show some kind of artificial broadening in the GGA calculation; on the other hand, they appear explicitly more localized in GGA-1/2 calculations.

We now explore the Mn-*d* projected DOS shown in Fig. 3. This DOS presents a peak slightly above the top of the spin-down valence band, and another more pronounced peak located at about 3 eV below the valence band edge. It is interesting to compare the position of this last peak with available experimental data. Usually the measured peak is referenced to the Fermi level. The first measurement was performed in 1999 by Okabayashi *et al.*<sup>29</sup> by means of a photoemission experiment employing photons in the energy range of 46–55 eV. They obtained a peak position of 4.5 eV below the Fermi level. This measurement was further confirmed by another experiment reported in 2001 also performed by Okabayashi *et al.*<sup>30</sup> Nevertheless, in 2002, a value of 3.5 eV was obtained by Åsklund *et al.*<sup>31</sup> using a photoemission experiment as well but with a photon energy of 81 eV, well above the resonant range for Mn. In 2004, the same group,<sup>32</sup> using the same technique, measured 3.7 eV for this peak and 4.7 eV for annealed samples at 430 °C. The 3.7 eV peak was then associated with substitutional Mn, whereas the other one was due to Mn in an interstitial position. In Table II, we compare our results with the experimental ones. We observe that the GGA-1/2 prediction has a better agreement with the most recent data in comparison to GGA.

In Table II, for a better comparison, we also display other theoretical results, obtained with different approaches for the XC potential. In 2010, Sato *et al.* published a review<sup>25</sup> where they predict the peak to appear at 5.2 eV below the Fermi level. This calculation was done using the pseudo-self-interaction (PSIC) scheme and a Mn concentration of 5%. They also report a result of 2.7 eV for a standard LDA calculation. In 2009, by employing the GGA+U method, AlZahrani *et al.* obtained the value of 3.4 eV, in

TABLE II. Position of Mn-*d* level (eV) inside the valence band referenced to the Fermi level.

Method	Value
GGA <sup>a</sup>	2.9
GGA-1/2 <sup>a</sup>	3.3
LDA	2.5 <sup>b</sup> ; 2.7 <sup>c</sup>
PSIC	5.2 <sup>c</sup>
GGA+U	3.4 <sup>d</sup>
SIC	3.16 <sup>e</sup> ; 3.23 <sup>e</sup>
OEP	3.7 <sup>e</sup>
LDA+U	4.2 <sup>f</sup>
Experimental	3.5 <sup>g</sup> ; 3.7 <sup>h</sup> ; 4.5 <sup>i</sup>

<sup>a</sup>This work.

<sup>b</sup>Reference 27.

<sup>c</sup>Reference 25.

<sup>d</sup>Reference 40.

<sup>e</sup>Reference 26.

<sup>f</sup>Reference 16.

<sup>g</sup>Reference 31.

<sup>h</sup>Reference 32.

<sup>i</sup>References 29 and 30.

well agreement with the experimental results of Refs. 31 and 32. In 2007, Schulthess *et al.*<sup>26</sup> employed the SIC approach to obtain this level in Ga<sub>0.9375</sub>Mn<sub>0.0625</sub>As, reaching 3.16 and 3.23 eV by two different calculations; they also employed a SIC based optimized effective potential (OEP) being able to achieve 3.7 eV. In 2004, Shick *et al.*<sup>16</sup> employed LDA+U to improve the LDA predictions and for  $U=4$  eV they got  $\sim 4.3$  eV for the distance between the Fermi level and the Mn-*d* main peak in the valence band; however, for different values of  $U$ , the position of the peak was altered (for  $U$  equal to 9 and 12 eV, they got  $\sim 6.5$  and  $\sim 8.3$  eV, respectively, for the position of this peak). They have also observed that the position of the Mn-*d* main peak is almost composition independent, contradicting some experimental results.<sup>31</sup>

Now we focus our attention on the band gap dependence on the Mn content. We vary the composition of Mn of Ga<sub>1-x</sub>Mn<sub>x</sub>As from  $x=0$  to  $x=0.25$  by changing the size of supercell employed in the calculations. For  $x=0$ , we have the standard GaAs, and for  $x=0.0625$ , 0.125, and 0.25, we use supercells with 32, 16, and 8 atoms, respectively, and in each supercells we replace one atom of Ga by one Mn. For each concentration, we calculate the spin-up band gap. This information can be used in the design of spintronic devices.<sup>33</sup> We consider this band gap as the energy difference between the lowest spin-up conduction band state (well above the Fermi level) and the highest spin-up state in the valence band (slightly above the Fermi level). In Fig. 4, we plot these results and compare them with other theoretical calculations and also with some experimental measurements available for small Mn composition. The values of Dietl *et al.*<sup>34</sup> and Tsuruoka *et al.*,<sup>35</sup> published in 2001 and 2002, respectively, show deviations of about 0.2 eV from the GGA-1/2 curve. We could observe the same deviation from the AlZahrani theoretical results based on GGA approach (albeit, the point shown refers to the minority spin band gap). When we consider the more recent experimental measurements, published in 2007 and 2011 by Thomas *et al.*<sup>36</sup> and Yastrubchak



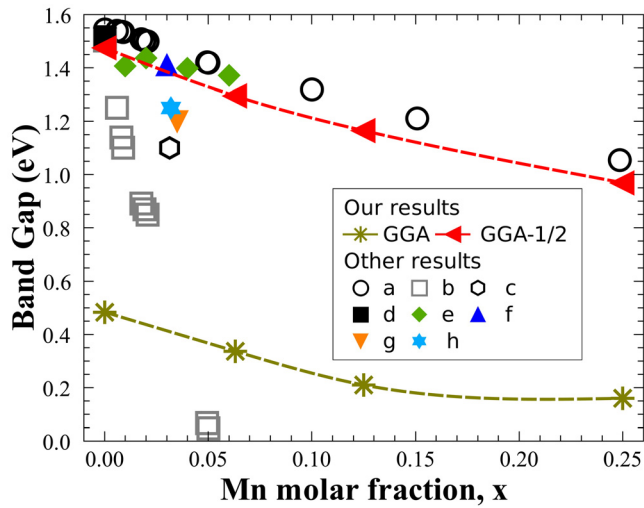


FIG. 4. Majority spin band gap of  $\text{Ga}_{1-x}\text{Mn}_x\text{As}$  from GGA and GGA-1/2 calculations compared with other results from a broad source of references. For the band gaps taken from literature, the open symbols come from theoretical calculations and the filled ones, from experimental measurements. Legend: *a* and *b*: Ref. 33 (methods A and B, respectively); *c*: Ref. 40 (this is a result for the minority spin band gap); *d*: Ref. 23; *e*: Ref. 37; *f*: Ref. 36; *g*: Ref. 34; *h*: Ref. 35.

et al.,<sup>37</sup> respectively, a very good agreement is seen between the theoretical and experimental results. Our GGA-1/2 findings are also endorsed by the theoretical calculations of Turek et al.,<sup>33</sup> performed in a tight-binding framework.

In order to provide an analytical expression for the energy band gap which could be of practical use and of easy access, we fit a second order polynomial curve to our results, and obtain the expression given in Eqs. (1) and (2), respectively, for GGA and GGA-1/2 gaps.

$$E_g(x) = 0.49 - 3.0x + 6.7x^2. \quad (1)$$

$$E_g(x) = 1.55 - 3.0x + 3.9x^2. \quad (2)$$

We stress that these expressions are valid only for small concentration of Mn once the expression obtained by fitting the full compositional range may differ from that obtained by fitting just a small interval of compositions.<sup>38</sup> From Eqs. (1) and (2), we get the bowing parameter for the band gap of this alloy: the GGA and GGA-1/2 values are 6.7 and 3.9 eV, respectively. Unfortunately, there is no experimental value for the bowing parameter.

In summary, we have studied theoretically the GaMnAs MS within the GGA-1/2 approach, calculating the position of Mn-*d* states and the band gap for small Mn concentrations. We obtained a good agreement between our results and the most recent experimental values reported for this material. From the calculated energy gap we derived an expression for  $E_g$ , and determined the band gap bowing for this MS. These calculations, in addition to other ones done before,<sup>39</sup> show that the GGA-1/2 technique can indeed be used to describe magnetic systems, opening a window to explore other relevant MSs such as GaMnN, InMnN, InMnAs, ZnCoO, ZnCrO, etc.

The authors are grateful for support by the Brazilian Funding Agencies FAPESP (2006/05858-0 and 2008/11423-1) and CNPq.

- <sup>1</sup>R. R. Pelá and L. K. Teles, *J. Magn. Magn. Mater.* **321**, 984 (2009).
- <sup>2</sup>R. R. Pelá and L. K. Teles, *J. Supercond. Novel Magn.* **23**, 61 (2010).
- <sup>3</sup>C. Caetano, L. K. Teles, M. Marques, and L. G. Ferreira, *J. Appl. Phys.* **107**, 123904 (2010).
- <sup>4</sup>A. H. Macdonald, P. Schiffer, and N. Samarth, *Nat. Mater.* **4**, 195 (2005).
- <sup>5</sup>T. Dietl, *Nat. Mater.* **9**, 965 (2010).
- <sup>6</sup>S. Pearton, *Nat. Mater.* **3**, 203 (2004).
- <sup>7</sup>A. Stroppa and G. Kresse, *Phys. Rev. B* **79**, 201201 (2009).
- <sup>8</sup>T. Jungwirth, J. Sinova, J. Masek, J. Kucera, and A. H. MacDonald, *Rev. Mod. Phys.* **78**, 809 (2006).
- <sup>9</sup>M. S. Hybertsen and S. G. Louie, *Phys. Rev. Lett.* **55**, 1418 (1985).
- <sup>10</sup>J. P. Perdew and A. Zunger, *Phys. Rev. B* **23**, 5048 (1981).
- <sup>11</sup>A. D. Becke, *J. Chem. Phys.* **98**, 1372 (1993).
- <sup>12</sup>R. Asahi, W. Mannstadt, and A. J. Freeman, *Phys. Rev. B* **59**, 7486 (1999).
- <sup>13</sup>M. Städele, J. A. Majewski, P. Vogl, and A. Görling, *Phys. Rev. Lett.* **79**, 2089 (1997).
- <sup>14</sup>V. I. Anisimov, F. Aryasetiawan, and A. I. Lichtenstein, *J. Phys.: Condens. Matter* **9**, 767 (1997).
- <sup>15</sup>F. Kwen, R. Leitsmann, and F. Bechstedt, *Phys. Rev. B* **80**, 045203 (2009).
- <sup>16</sup>A. B. Shick, J. Kudrnovský, and V. Drchal, *Phys. Rev. B* **69**, 125207 (2004).
- <sup>17</sup>L. G. Ferreira, M. Marques, and L. K. Teles, *Phys. Rev. B* **78**, 125116 (2008).
- <sup>18</sup>L. G. Ferreira, M. Marques, and L. K. Teles, *AIP Adv.* **1**, 032119 (2011).
- <sup>19</sup>R. R. Pelá, C. Caetano, M. Marques, L. G. Ferreira, J. Furthmüller, and L. K. Teles, *Appl. Phys. Lett.* **98**, 151907 (2011).
- <sup>20</sup>M. Ribeiro, Jr., L. R. C. Fonseca, and L. G. Ferreira, *Phys. Rev. B* **79**, 241312 (2009).
- <sup>21</sup>G. Kresse and J. Hafner, *Phys. Rev. B* **47**, R558 (1993).
- <sup>22</sup>G. Kresse and J. Furthmüller, *Comput. Mater. Sci.* **6**, 15 (1996).
- <sup>23</sup>I. Vurgaftman, J. R. Meyer, and L. R. Ram-Mohan, *J. Appl. Phys.* **89**, 5815 (2001).
- <sup>24</sup>H. Ohno, A. Shen, F. Matsukura, A. Oiwa, A. Endo, S. Katsumoto, and Y. Iye, *Appl. Phys. Lett.* **69**, 363 (1996).
- <sup>25</sup>K. Sato, L. Bergqvist, J. Kudrnovský, P. H. Dederichs, O. Eriksson, I. Turek, B. S. Bouzerar, G. Bouzerar, H. Katayama-Yoshida, V. A. Dinh, T. Fukushima, H. Kizaki, and R. Zeller, *Rev. Mod. Phys.* **82**, 1633 (2010).
- <sup>26</sup>T. C. Schulthess, W. M. Temmerman, Z. Szotek, A. Svane, and L. Petit, *J. Phys.: Condens. Matter* **19**, 165207 (2007).
- <sup>27</sup>L. Bergqvist, P. A. Korzhavyi, B. Sanyal, S. Mirbt, I. A. Abrikosov, L. Nordström, E. A. Smirnova, P. Mohn, P. Svedlindh, and O. Eriksson, *Phys. Rev. B* **67**, 205201 (2003).
- <sup>28</sup>S. Sanvito, P. Ordejón, and N. A. Hill, *Phys. Rev. B* **63**, 165206 (2001).
- <sup>29</sup>J. Okabayashi, A. Kimura, T. Misokawa, A. Fujimori, T. Hayashi, and M. Tanaka, *Phys. Rev. B* **59**, R2486 (1999).
- <sup>30</sup>J. Okabayashi, A. Kimura, O. Rader, T. Misokawa, A. Fujimori, T. Hayashi, and M. Tanaka, *Phys. Rev. B* **64**, 125304 (2001).
- <sup>31</sup>H. Åsklund, L. Ilver, J. Kanski, J. Sadowski, and R. Mathieu, *Phys. Rev. B* **66**, 115319 (2002).
- <sup>32</sup>M. Adell, L. Ilver, J. Kanski, J. Sadowski, R. Mathieu, and V. Stanciu, *Phys. Rev. B* **70**, 125204 (2004).
- <sup>33</sup>M. Turek, J. Siewert, and J. Fabian, *Phys. Rev. B* **78**, 085211 (2008).
- <sup>34</sup>T. Dietl, H. Ohno, and F. Matsukura, *Phys. Rev. B* **63**, 195205 (2001).
- <sup>35</sup>T. Tsuruoka, N. Tachikawa, S. Ushioda, F. Matsukura, K. Takamura, and H. Ohno, *Appl. Phys. Lett.* **81**, 2800 (2002).
- <sup>36</sup>O. Thomas, O. Makarovskiy, A. Patan, L. Eaves, R. P. Campion, K. W. Edmonds, C. T. Foxon, and B. L. Gallagher, *Appl. Phys. Lett.* **90**, 082106 (2007).
- <sup>37</sup>O. Yastrubchak, J. Żuk, H. Krzyanowska, J. Z. Domagala, T. Andrearczyk, J. Sadowski, and T. Wosinski, *Phys. Rev. B* **83**, 245201 (2011).
- <sup>38</sup>C. Caetano, L. K. Teles, M. Marques, A. Dal Pino, Jr, and L. G. Ferreira, *Phys. Rev. B* **74**, 045215 (2006).
- <sup>39</sup>A. Belabbes, A. Zaoui, and M. Ferhat, *Appl. Phys. Lett.* **97**, 242509 (2010).
- <sup>40</sup>A. Z. AlZahrani, G. P. Srivastava, R. Garg, and M. A. Migliorato, *J. Phys.: Condens. Matter* **21**, 485504 (2009).